

Electronic supplementary information

Evaluating the energy landscape of an out-of-equilibrium bistable [2]rotaxane containing monopyrrolotetrathiafulvalene

Mathias S. Neumann,^a Amanda F. Smith,^a Sofie K. Jensen,^a Rikke Frederiksen,^a
Mathias L. Skavenborg^a and Jan O. Jeppesen^{a*}

^a*Department of Physics, Chemistry and Pharmacy, University of Southern Denmark,
Campusvej 55, 5230 Odense, Denmark. E-mail: joj@sdu.dk*

Table of contents

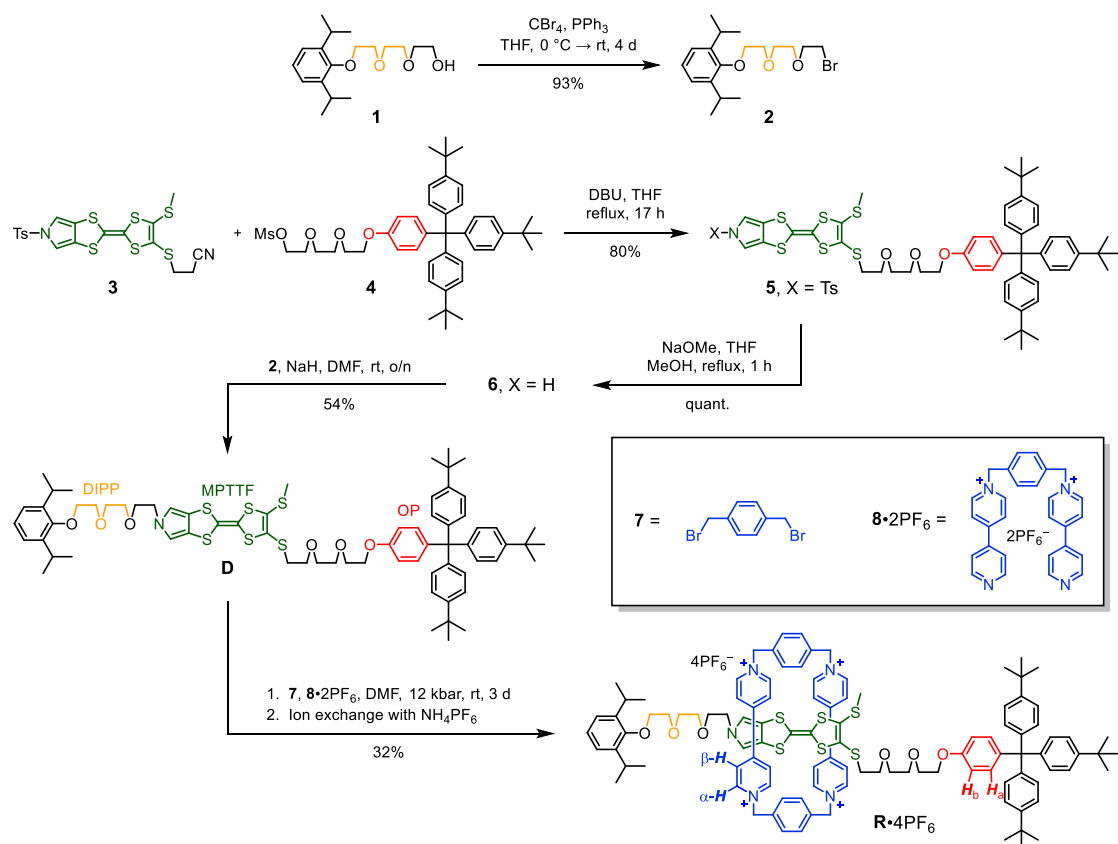
1	Experimental details.....	S2
1.1	General methods	S2
1.2	Synthesis of the [2]rotaxane R •4PF ₆	S3
1.3	Synthesis and characterisation of [2]rotaxane R •DIPP ⁶⁺ and [2]rotaxane R •OP ⁶⁺	S7
2	Photophysical characterisation of CBPQT ⁴⁺ , D and R ⁴⁺	S8
3	¹ H NMR investigations of the [2]rotaxane R ⁴⁺	S9
4	¹ H NMR spectra of R ⁴⁺ , R •DIPP ⁶⁺ and R •OP ⁶⁺	S10
5	2D NMR spectra of D , R ⁴⁺ and R •OP ⁶⁺	S11
6	Electrochemical characterisation.....	S13
7	¹ H NMR kinetic experiment carried out on R ⁶⁺	S14
8	First-order analysis of the NMR kinetic experiment	S15
9	Determination of rate constants by the numerical method.....	S16
9.1	Results from MATLAB calculation on R ⁶⁺ at 298 K.....	S19
10	¹ H NMR and ¹³ C NMR spectra	S22
11	References	S25

1 Experimental details

1.1 General methods

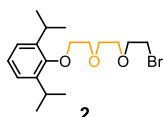
All chemicals are commercially available and were used as received unless otherwise stated. The compounds 2-(2-(2-(2,6-diisopropylphenoxy)ethoxy)ethoxy)ethan-1-ol^{S1} (**1**), 2-[4-(2-cyanoethylthio)-5-methylthio-1,3-dithiole-2-yliden]-5-tosyl-(1,3)-dithiolo[4,5-*c*]pyrrole^{S2} (**3**), 2-(2-(2-[4-(tris(4-*t*-butylphenyl)methyl)phenoxy]ethoxy)ethoxy)ethyl methanesulfonate^{S3} (**4**) and 1''-[1,4-phenylene-bis(methylene)]bis(4,4'-bipyridinium) bis(hexafluorophosphate)^{S4} (**8**•2PF₆) were all prepared according to literature procedures. All reactions were carried out under an anhydrous nitrogen atmosphere. CH₂Cl₂ was distilled prior to use. THF was distilled from molecular sieves (4 Å) and deperoxide sieves and MeOH was dried over molecular sieves (3 Å) prior to use. DMF was dried over molecular sieves (4 Å) prior to use. The high-pressure reaction was performed in a custom-made Teflon tube, using a Psika high-pressure apparatus. Thin-layer chromatography (TLC) was carried out using aluminium sheets precoated with SiO₂ (Merck 60 F254) and visualised with UV light (254 nm) or I₂ vapour. Column chromatography was carried out using SiO₂ (Merck 60 F 0.040–0.063 mm). ¹H NMR spectra were recorded at 298 K at 400 or 500 MHz, on a 400 MHz Bruker AVANCE-III spectrometer or a 500 MHz JEOL JNM-ECZR spectrometer using residual non-deuterated solvent as the internal standard. The solvent signals were assigned using Gottlieb *et al.*^{S5} The following abbreviations are used in listing the NMR spectra: s = singlet, bs = broad singlet, d = doublet, t = triplet, q = quartet and m = multiplet. Melting points (Mp) were determined on a Büchi 353 melting point apparatus and are uncorrected. Electrospray ionisation mass spectrometry (ESI-MS) was performed on a Bruker Daltonics MicrOTOF-Q II ESI-Qq-TOF mass spectrometer. UV-Vis-NIR spectroscopic data were recorded on an Agilent Cary 5000 spectrophotometer. Cyclic voltammetry (CV) was carried out on an Autolab PGSTAT30 potentiostat. The CV cell consisted of a glassy carbon working electrode (WE), a Pt wire counter electrode (CE), and an Ag/AgNO₃ reference electrode (RE). The measurements were carried out in MeCN with *n*-Bu₄N•PF₆ (0.1 M) as the electrolyte and with a scan rate of 100 mV s⁻¹ at 298 K. The WE was polished with an Al₂O₃ slurry prior to use and all solutions were degassed (N₂) prior to use. All redox potentials were measured against Ag/Ag⁺ and converted into vs. ferrocene/ferrocenium (Fc/Fc⁺). Elemental analyses were performed by Atlantic Microlabs, Inc., Norcross, GA, USA.

1.2 Synthesis of the [2]rotaxane R•4PF₆



Scheme S1 Synthesis of the [2]rotaxane R•4PF₆.

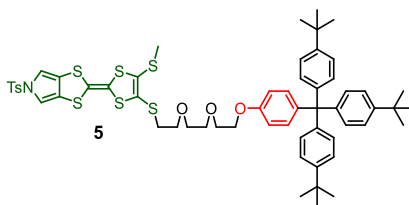
2-(2-(2-(2-Bromoethoxy)ethoxy)ethoxy)-1,3-diisopropylbenzene^{S6} (2)



Triphenylphosphine (11.5 g, 43.8 mmol) was added in small portions over a period of 1 h to a stirred solution of the 2-(2-(2-(2,6-diisopropylphenoxy)ethoxy)ethoxy)ethan-1-ol (**1**) (6.04 g, 19.4 mmol) and CBr₄ (9.82 g, 29.6 mmol) in anhydrous THF (100 mL) at 0 °C. The reaction mixture was allowed to reach rt and then stirred for 4 d at rt before it was filtered through celite (200 mL). The filter was washed with anhydrous THF (500 mL) and the combined filtrate was concentrated to give a brown oil, which was redissolved in CH₂Cl₂ (150 mL), washed with H₂O (2 × 150 mL) and dried (MgSO₄). The solvent was evaporated, and the residue was purified by column chromatography (600 mL SiO₂, 8 cm Ø, CH₂Cl₂). The colourless band (*R_f* = 0.5) was collected and concentrated to afford compound **2** as a clear yellow oil (6.74 g, 18.1 mmol, 93%). ¹H NMR (400 MHz, CDCl₃, 298 K): δ (ppm) = 1.22 (d, *J* = 6.9 Hz, 12H, CH(CH₃)₂), 3.38 (sept, *J* = 6.9 Hz, 2H, CH(CH₃)₂), 3.50 (t, *J* = 6.3 Hz, 2H, CH₂Br),

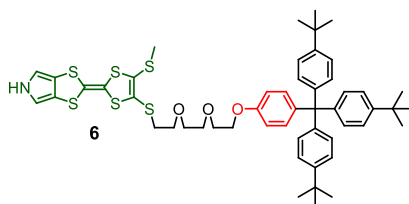
3.72–3.80 (m, 4H, CH₂O), 3.83–3.89 (m, 4H, CH₂O), 3.90–3.94 (m, 2H, CH₂O), 7.10 (s, 3H, Ar-H). ¹³C NMR (100 MHz, CDCl₃, 298 K): δ (ppm) = 24.3 (CH(CH₃)₂), 26.4 (CH(CH₃)₂), 30.4 (CH₂Br), 70.8 (CH₂O), 70.9 (CH₂O), 71.2 (CH₂O), 71.5 (CH₂O), 74.0 (CH₂O), 124.2 (Ar-CH), 124.8 (Ar-CH), 142.0 (Ar-C), 153.2 (Ar-C). MS (ESI): *m/z* = 395 [M+Na]⁺; 397 [M+2+Na]⁺. MS (HiRes-FT ESI) calcd. for C₁₈H₂₉BrNaO₃⁺: 395.1192; found: 395.1208. Anal. calcd. for C₁₈H₂₉BrO₃: C, 57.91; H, 7.83; found: C, 57.95; H, 7.79.

MPTTF derivative 5



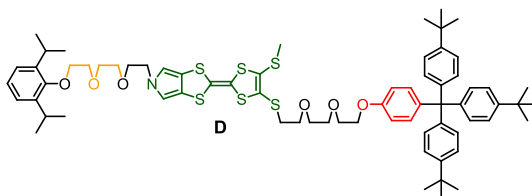
2-[4-(2-Cyanoethylthio)-5-methylthio-1,3-dithiole-2-ylidene]-5-tosyl-(1,3)-dithiolo[4,5-*c*]pyrrole (**3**) (409 mg, 774 μmol) and 2-(2-(2-[4-(tris(4-*t*-butylphenyl)methyl)phenoxy]ethoxy)ethoxy)ethyl methanesulfonate (**4**) (526 mg, 735 μmol) were dissolved in anhydrous THF (80 mL) and degassed (N₂, 15 min) before DBU (0.25 mL, 255 mg, 1.67 mmol) was added. The reaction mixture was heated under reflux for 17 h and cooled to rt before the solvent was removed under reduced pressure. The brown residue was purified by column chromatography (250 mL SiO₂, 5.5 cm Ø, eluent: CH₂Cl₂). The orange band (*R_f* = 0.7, CH₂Cl₂) was collected, and the solvent evaporated which gave compound **5** as a yellow solid (642 mg, 587 μmol, 80%). Mp 149.8–153.9 °C. ¹H NMR (CDCl₃, 400 MHz, 298 K): δ (ppm) = 1.30 (s, 27H, C(CH₃)₃), 2.38 (s, 3H, Ts-CH₃), 2.40 (s, 3H, SCH₃), 2.98 (t, *J* = 6.7 Hz, 2H, SCH₂), 3.62–3.72 (m, 6H, CH₂O), 3.81–3.85 (m, 2H, CH₂O), 4.06–4.11 (m, 2H, CH₂O), 6.77 (d, *J* = 8.8 Hz, 2H, OP-*H_b*), 6.91 (s, 2H, pyrrole-*H*), 7.07 (d, *J* = 8.8 Hz, 8H, Ar-*H* + OP-*H_a*), 7.23 (d, *J* = 8.8 Hz, 6H, Ar-*H*), 7.28 (d, *J* = 8.3 Hz, 2H, Ts-Ar-*H*), 7.71 (d, *J* = 8.3 Hz, 2H, Ts-Ar-*H*). MS (ESI): *m/z* = 1093 [M]⁺, 1116 [M+Na]⁺. MS (HiRes-FT ESI) calcd. for C₅₉H₆₇NNaO₅S₇⁺: 1116.2956; found: 1116.2925. Anal. calcd. for C₅₉H₆₇NO₅S₇: C, 64.74; H, 6.17; N, 1.28; S, 20.50; found: C, 64.76; H, 6.08; N, 1.35; S, 20.67.

MPTTF derivative 6



The MPTTF derivative **5** (182 mg, 166 μmol) was dissolved in anhydrous THF/MeOH (1:1, 50 mL) and degassed (N_2 , 15 min). A solution of NaOMe in MeOH (0.38 mL, 25% w/v, 1.66 mmol) was added, and the solution was heated to reflux for 1 h before it was cooled to rt. The solvent was removed under reduced pressure, and the brown residue was redissolved in CH_2Cl_2 (75 mL) and washed with H_2O (3×50 mL). The organic phase was dried (MgSO_4) and concentrated under reduced pressure affording the MPPTF compound **6** as a yellow solid. (158 mg, 168 μmol , quant.). Mp 201.9–203.6 $^\circ\text{C}$. ^1H NMR (400 MHz, CDCl_3 , 298 K): δ (ppm) = 1.30 (s, 27H, $\text{C}(\text{CH}_3)_3$), 2.41 (s, 3H, SCH_3), 3.00 (t, $J = 6.6$ Hz, 2H, SCH_2), 3.64–3.73 (m, 6H, CH_2O), 3.83 (dd, $J = 5.7, 4.0$ Hz, 2H, CH_2O), 4.07 (dd, $J = 5.7, 4.0$ Hz, 2H, CH_2O), 6.50–6.53 (m, 2H, pyrrole-*H*), 6.74 (d, $J = 8.9$ Hz, 2H, OP-*H*_b), 7.04 (d, $J = 8.9$ Hz, 2H, OP-*H*_a), 7.08 (d, $J = 8.6$ Hz, 6H, Ar-*H*), 7.23 (d, $J = 8.6$ Hz, 6H, Ar-*H*), 7.98 (bs, 1H, pyrrole-NH). MS (ESI): $m/z = 939$ [M]⁺, 957 [$\text{M}+\text{NH}_4$]⁺, 962 [$\text{M}+\text{Na}$]⁺. MS (HiRes-FT ESI): calcd for $\text{C}_{52}\text{H}_{61}\text{NO}_3\text{S}_6$ ⁺: 939.2971; found: 939.2994. Anal. Calcd for $\text{C}_{52}\text{H}_{61}\text{NO}_3\text{S}_6$; C, 66.41; H, 6.54; N, 1.49; S, 20.45; found: C, 66.49; H, 6.58; N, 1.55; S, 20.18.

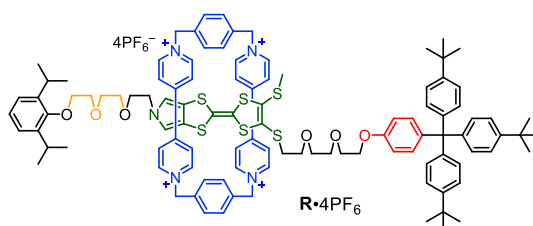
Dumbbell D



The MPTTF derivative **6** (108 mg, 115 μmol) and 2-(2-(2-(2-bromoethoxy)ethoxy)ethoxy)-1,3-diisopropylbenzene (**2**) (65.2 mg, 174 μmol) were dissolved in anhydrous DMF (15 mL) and degassed (N_2 , 15 min) before NaH (60% w/w dispersion in mineral oil, 38.4 mg, 960 μmol) was added. The reaction mixture was stirred overnight at rt before the reaction mixture was carefully quenched by the addition of H_2O (5 mL), whereupon it was concentrated under reduced pressure. The residue was redissolved in CH_2Cl_2 (100 mL), washed with brine (2×100 mL) and H_2O (2×100 mL) before being dried (MgSO_4). Removal of the solvent gave a brown residue, which was purified by column chromatography (150 mL SiO_2 , 4 cm \varnothing , eluent: CH_2Cl_2). The yellow band ($R_f = 0.2$) was collected and concentrated to yield the dumbbell **D** as a yellow solid (75.1 mg,

61.7 μmol , 54%). Mp 57.9–59.1 $^{\circ}\text{C}$. $^1\text{H NMR}$ (500 MHz, CDCl_3 , 298 K): δ (ppm) = 1.22 (d, $J = 6.9$ Hz, 12H, $\text{CH}(\text{CH}_3)_2$), 1.29 (s, 27H, $\text{C}(\text{CH}_3)_3$), 2.40 (s, 3H, SCH_3), 2.99 (t, $J = 6.6$ Hz, 2H, SCH_2), 3.37 (sept, $J = 6.9$ Hz, 2H, $\text{CH}(\text{CH}_3)_2$), 3.59–3.77 (m, 12H, CH_2O), 3.78–3.87 (m, 4H, CH_2O), 3.91 (dd, $J = 5.2, 4.3$ Hz, 2H, CH_2O), 3.97 (t, $J = 5.3$ Hz, 2H, CH_2O), 4.09 (t, $J = 4.9$, 2H, NCH_2), 6.51 and 6.52 (AB, $J_{\text{AB}} = 2.1$ Hz, 2H, pyrrole- H), 6.77 (d, $J = 8.9$ Hz, 2H, OP- H_b), 7.03–7.12 (m, 11H, OP- H_a + Ar- H), 7.22 (d, $J = 8.6$ Hz, 6H, Ar- H). $^1\text{H NMR}$ (400 MHz, CD_3CN , 298 K): δ (ppm) = 1.17 (d, $J = 6.9$ Hz, 12H, $\text{CH}(\text{CH}_3)_2$), 1.28 (s, 27H, $\text{C}(\text{CH}_3)_3$), 2.37 (s, 3H, SCH_3), 2.96 (t, $J = 6.2$ Hz, 2H, SCH_2), 3.37 (sept, $J = 6.9$ Hz, 2H, $\text{CH}(\text{CH}_3)_2$), 3.51–3.65 (m, 10H, CH_2O), 3.65–3.75 (m, 6H, CH_2O), 3.80–3.86 (m, 2H, CH_2O), 3.97 (t, $J = 5.0$ Hz, 2H, CH_2O), 4.00–4.07 (m, 2H, NCH_2), 6.64 and 6.65 (AB, $J_{\text{AB}} = 2.1$ Hz, 2H, pyrrole- αH), 6.78 (d, $J = 9.0$ Hz, 2H, Ar- H_b), 7.04–7.13 (m, 5H, Ar- H_a + Ar- H), 7.15 (d, $J = 8.7$ Hz, 6H, Ar- H), 7.30 (d, $J = 8.7$ Hz, 6H, Ar- H). MS (ESI): $m/z = 1231$ [M] $^+$, 1232 [$\text{M}+\text{H}$] $^+$, 1250 [$\text{M}+\text{NH}_4$] $^+$, 1254 [$\text{M}+\text{Na}$] $^+$. MS (HiRes-FT ESI) calcd. For $\text{C}_{70}\text{H}_{90}\text{NO}_6\text{S}_6$ $^{+}$: 1232.5087; found: 1232.4901. Anal. Calcd for $\text{C}_{70}\text{H}_{89}\text{NO}_6\text{S}_6$: C, 68.20; H, 7.28; N, 1.14; found: C, 67.95; H, 7.20; N, 1.13.

[2]Rotaxane $\mathbf{R}\cdot 4\text{PF}_6$

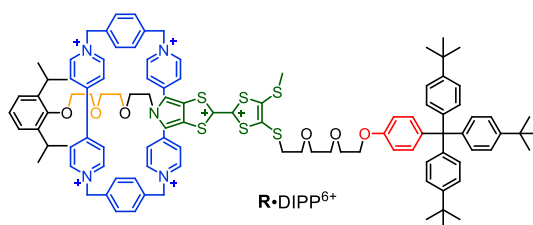


The dumbbell **D** (106 mg, 85.8 μmol), 1,4-bis(bromomethyl)benzene (**7**) (89.0 mg, 337 μmol) and 1,1''-[1,4-phenylene-bis(methylene)]bis(4,4'-bipyridinium) bis(hexafluorophosphate) (**8**·2PF₆) (228 mg, 323 μmol) were dissolved in anhydrous DMF (5 mL) and transferred to a Teflon tube, which was subjected to 12 kbar pressure for 3 d at rt. The resulting green reaction mixture was purified by column chromatography (75 mL SiO₂, 3 cm \varnothing). Unreacted dumbbell **D** was eluted with Me₂CO, where after the eluent was changed to Me₂CO/NH₄PF₆ (100:0.25 (v/w)) and the green band was collected. Most of the solvent was removed under reduced pressure and cold H₂O (5 $^{\circ}\text{C}$, 75 mL) was added. The resulting precipitate was collected by filtration, washed with H₂O (5 \times 2 mL) and Et₂O (3 \times 2 mL) before being dried to yield the [2]rotaxane $\mathbf{R}\cdot 4\text{PF}_6$ as a green solid (63.5 mg, 27.2 μmol , 32%). Mp 200–230 $^{\circ}\text{C}$ (dec. without melting). $^1\text{H NMR}$ (500 MHz, CD_3CN , 298 K): δ (ppm) = 1.12 (d, $J = 6.9$ Hz, 12H, $\text{CH}(\text{CH}_3)_2$), 1.28 (s, 27H, $\text{C}(\text{CH}_3)_3$), 2.67 (s, 3H, SCH_3), 3.19–3.29 (m, 4H, SCH_2 + $\text{CH}(\text{CH}_3)_2$), 3.72–3.88 (m, 14H, CH_2O), 3.90 (t, $J = 6.2$ Hz, 2H, CH_2O), 3.95 (t, $J = 5.1$ Hz, 2H, CH_2O), 4.01 (m, 2H, CH_2O), 4.11 (t, $J = 5.1$ Hz, 2H, NCH_2), 5.70 and 5.73 (AB, $J_{\text{AB}} = 13.7$ Hz, 8H, CBPQT⁴⁺-

N^+CH_2), 6.21 and 6.24 (AB, $J_{AB} = 1.9$ Hz, 2H, pyrrole- H), 6.68 (d, $J = 8.9$ Hz, 2H, OP- H_b), 7.03–7.12 (m, 5H, OP- H_a + Ar- H), 7.15 (d, $J = 8.6$ Hz, 6H, Ar- H), 7.31 (d, $J = 8.6$ Hz, 6H, Ar- H), 7.73 (bs, 4H, CBPQT $^{4+}$ - βH), 7.76 (s, 4H, CBPQT $^{4+}$ -xylyl- H), 7.77 (s, 4H, CBPQT $^{4+}$ -xylyl- H), 8.01 (bs, 4H, CBPQT $^{4+}$ - βH), 8.83 (bs, 4H, CBPQT $^{4+}$ - αH), 9.01 (bs, 4H, bs, 4H, CBPQT $^{4+}$ - αH). MS (ESI): $m/z = 1021$ $[M-2PF_6]^{2+}$. MS (HiRes-FT-ESI) calcd. for $C_{106}H_{121}F_{12}N_5O_6P_2S_6^{2+}$: 1021.3474; found: 1021.3485. Anal. Calcd for $C_{106}H_{121}F_{24}N_5O_6P_4S_6$; C, 54.56; H, 5.23; N, 3.00; S, 8.24; found: C, 54.29; H, 5.35; N, 3.05; S, 8.02.

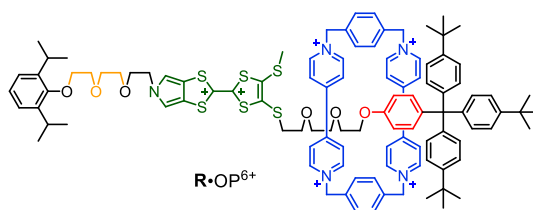
1.3 Synthesis and characterisation of [2]rotaxane $R \cdot DIPP^{6+}$ and [2]rotaxane $R \cdot OP^{6+}$

[2]Rotaxane $R \cdot DIPP^{6+}$



TBPASbCl $_6$ (10.4 mg, 12.8 μ mol) was added to a solution of the [2]rotaxane $R \cdot 4PF_6$ (2.98 mg, 1.28 μ mol) in CD $_3$ CN (640 μ L) at rt, whereafter a 1H NMR spectrum of the resulting $R \cdot DIPP^{6+}$ was recorded as fast as possible (ca. 5 min). 1H NMR (400 MHz, CD $_3$ CN, 298 K): δ (ppm) = 0.30 (bs, 2H, CH $_2$ O), 0.69 (bs, 2H, CH $_2$ O), 0.84 (bs, 2H, CH $_2$ O), 1.29 (s, 27H, C(CH $_3$) $_3$), 1.44 (d, $J = 6.9$ Hz, 12H, CH(CH $_3$) $_2$), 2.93 (bs, 3H, SCH $_3$), 3.21–4.09 (m, 20H, SCH $_2$ + CH(CH $_3$) $_2$ + NCH $_2$ + CH $_2$ O), 5.87 (bs, 8H, CBPQT $^{4+}$ -N $^+CH_2$), 6.76 (d, $J = 8.6$ Hz, 2H, OP- H_b), 7.16–7.37 (m, 17H, Ar- H + OP- H_a), 7.56–7.65 (m, 10H, pyrrole- H + CBPQT $^{4+}$ -xylyl- H), 8.30 (bs, 8H, CBPQT $^{4+}$ - βH), 9.00 (bs, 8H, CBPQT $^{4+}$ - αH).

[2]Rotaxane $R \cdot OP^{6+}$



The solution of [2]rotaxane $R \cdot DIPP^{6+}$ in CD_3CN was left to equilibrate for 80 min at rt, whereafter a 1H NMR spectrum of the resulting $R \cdot OP^{6+}$ was recorded. 1H NMR (400 MHz, CD_3CN , 298 K): δ (ppm) = 1.17 (d, $J = 6.9$ Hz, 12H, $CH(CH_3)_2$), 1.37 (s, 27H, $C(CH_3)_3$), 1.41–1.44 (m, 2H, CH_2O), 2.53 (d, $J = 8.6$ Hz, 2H, $OP-H_b$), 3.03 (s, 3H, SCH_3), 3.39 (sept, $J = 6.9$ Hz, 2H, $CH(CH_3)_2$)^{S7}, 3.42–3.46 (m, 2H, CH_2O)⁷, 3.61 (t, $J = 5.6$ Hz, 2H, SCH_2), 3.69 (s, 4H, CH_2O), 3.76–3.80 (m, 2H, CH_2O), 3.82–3.86 (m, 2H, CH_2O), 3.87–3.91 (m, 2H, CH_2O), 3.94–3.99 (m, 4H, CH_2O), 4.02 (t, $J = 5.6$ Hz, 2H, CH_2O), 4.60 (bs, 2H, NCH_2), 5.79 and 5.82 (AB, $J_{AB} = 13.5$ Hz, 8H, $CBPQT^{4+}-N^+CH_2$), 6.27 (d, $J = 8.6$ Hz, 2H, $OP-H_a$), 7.06–7.16 (m, 3H, $Ar-H$), 7.35 (d, $J = 8.4$ Hz, 6H, $Ar-H$), 7.53–7.65 (m, 14H, $Ar-H + CBPQT^{4+}-\beta H$), 7.67 (s, 8H, $CBPQT^{4+}-xylyl-H$), 8.15 (s, 2H, pyrrole- H), 8.85 (d, $J = 6.6$ Hz, 8H, $CBPQT^{4+}-\alpha H$).

2 Photophysical characterisation of $CBPQT^{4+}$, **D** and R^{4+}

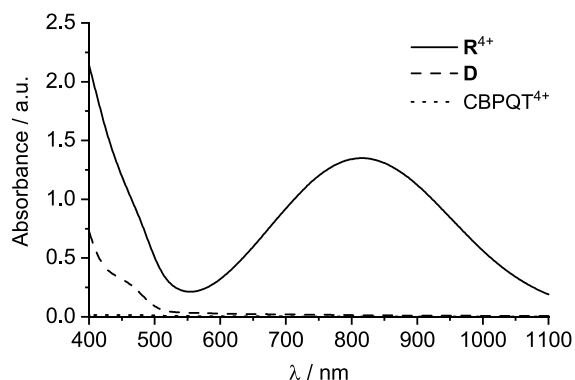


Fig. S1 UV/vis/NIR absorption spectra recorded of R^{4+} (0.8 mM), **D** (0.8 mM) and $CBPQT^{4+}$ (0.8 mM) recorded in MeCN at 298 K.

3 ^1H NMR investigations of the [2]rotaxane R^{4+}

A comparison of the ^1H NMR spectra (500 MHz) recorded in CD_3CN at 298 K of R^{4+} (Fig. S2b) and the corresponding dumbbell **D** (Fig. S2c) clearly reveals that CBPQT^{4+} is mechanically bonded to the dumbbell component in R^{4+} , because of the appearance of four broad singlets resonating at 7.73 (4H), 8.01 (4H), 8.81 (4H) and 9.00 (4H) ppm, a doublet resonating at 7.76 (8H) ppm and an AB system ($J_{\text{AB}} = 13.7$ Hz) resonating at 5.70 and 5.73 (8H) ppm, that can be associated with the $\alpha\text{-H}$ and $\beta\text{-H}$ protons, the xylyl- H protons and the N^+CH_2 protons, respectively, present in the CBPQT^{4+} ring. In addition, several of the resonances associated with the protons in the dumbbell component of R^{4+} are shifted relative to the same protons in the dumbbell **D** (Fig. S2c). For instance, the pyrrole- H protons resonate as an AB system ($J_{\text{AB}} = 1.9$ Hz) at 6.21 and 6.24 ppm in R^{4+} and are significantly upfield shifted ($\Delta\delta = -0.42$ ppm) compared to their position in the dumbbell **D**, on account of the shielding effect of CBPQT^{4+} that arise when CBPQT^{4+} encircles the MPTTF unit.^{S8} Furthermore, the protons associated with the SCH_3 group in R^{4+} are found resonating as a singlet at 2.67 ppm and have experienced a downfield shift ($\Delta\delta = +0.30$ ppm) relative to their position in the dumbbell **D**, a situation which is fully consistent with CBPQT^{4+} encircling an MPTTF unit.^{S8b}

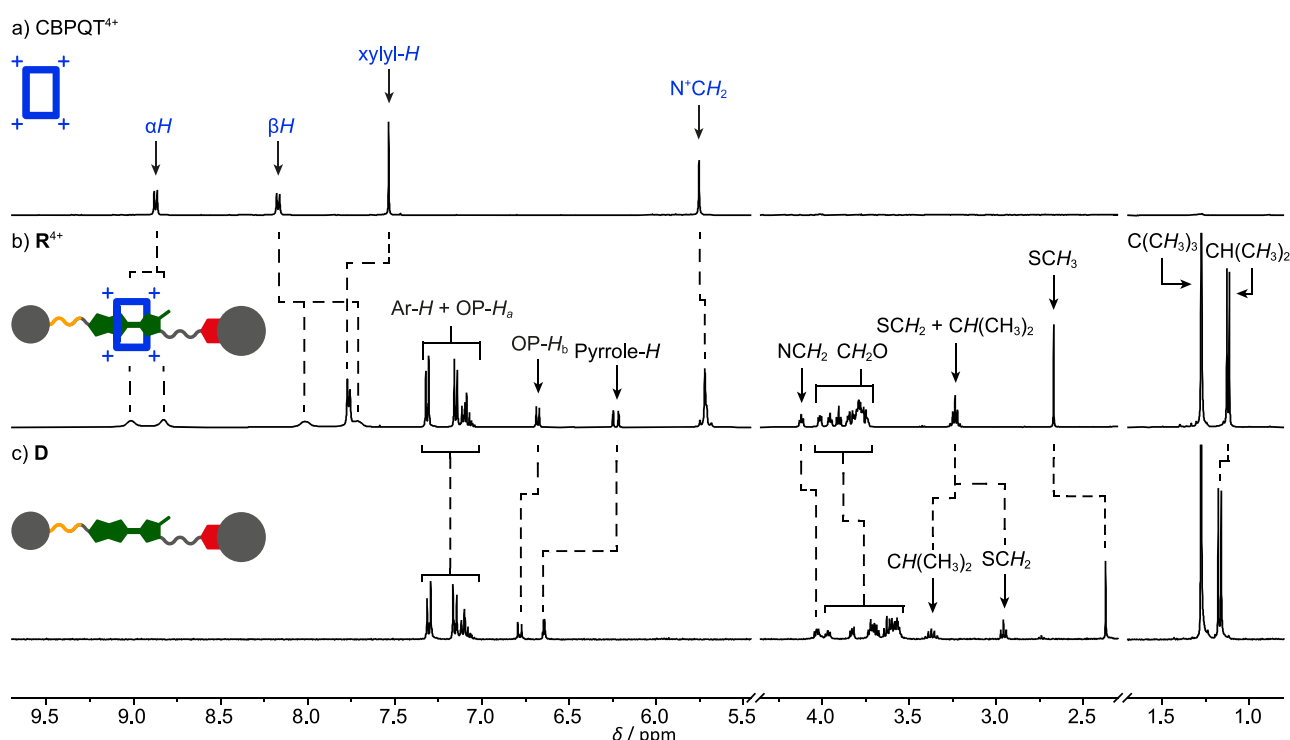


Fig. S2 Partial ^1H NMR spectra recorded in CD_3CN (2 mM) at 298 K of (a) CBPQT^{4+} (400 MHz), (b) [2]rotaxane R^{4+} (500 MHz) and (c) dumbbell **D** (400 MHz). Areas containing solvent residual peak and H_2O are omitted for clarity.

4 ^1H NMR spectra of R^{4+} , $\text{R}\cdot\text{DIPP}^{6+}$ and $\text{R}\cdot\text{OP}^{6+}$

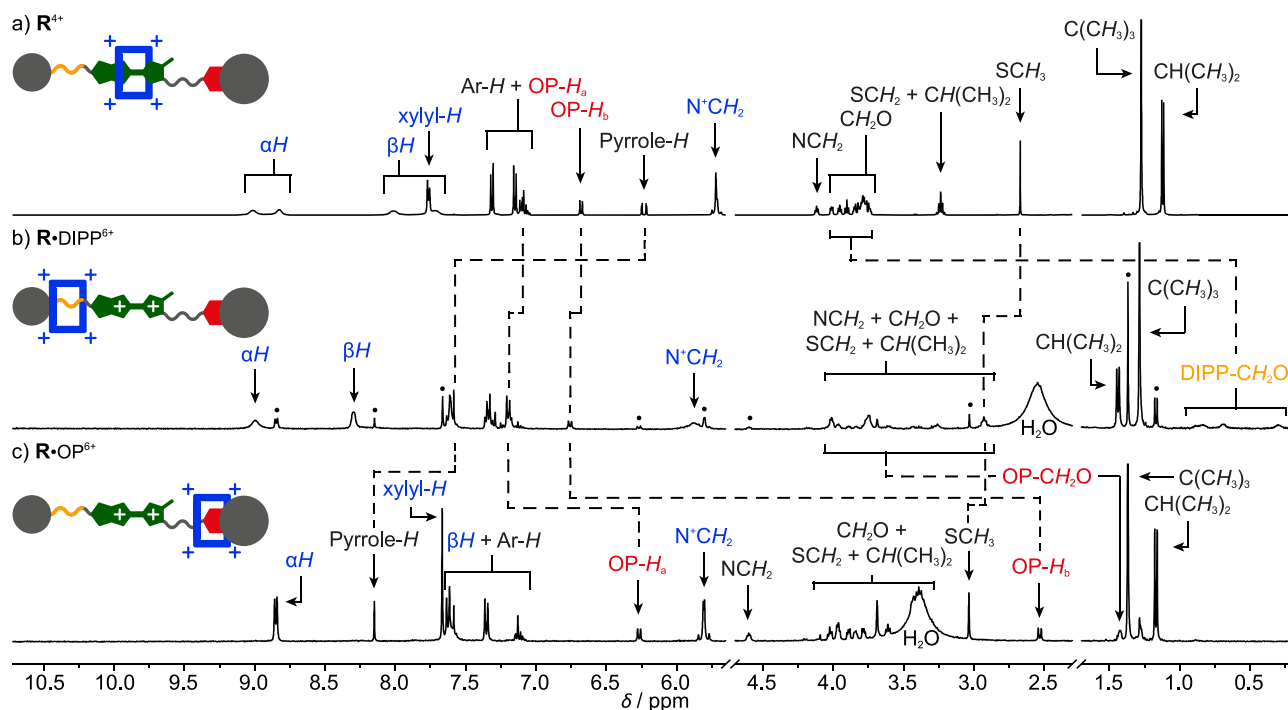


Fig. S3 Partial ^1H NMR spectra recorded in CD_3CN (2 mM) at 298 K of (a) [2]rotaxane R^{4+} (500 MHz), (b) oxidised [2]rotaxane R^{6+} (400 MHz) recorded ca. 5 min after addition of ten equiv. of TBPASbCl_6 and (c) oxidised [2]rotaxane R^{6+} (400 MHz) recorded 90 min after addition of TBPASbCl_6 . All signals in (b) can be associated with the protons in $\text{R}\cdot\text{DIPP}^{6+}$, except the signals marked with \bullet which can be associated with the protons in $\text{R}\cdot\text{OP}^{6+}$, while all signals in (c) can be associated with the protons in $\text{R}\cdot\text{OP}^{6+}$. Areas containing residual solvent peak are omitted for clarity.

5 2D NMR spectra of D, R⁴⁺ and R•OP⁶⁺

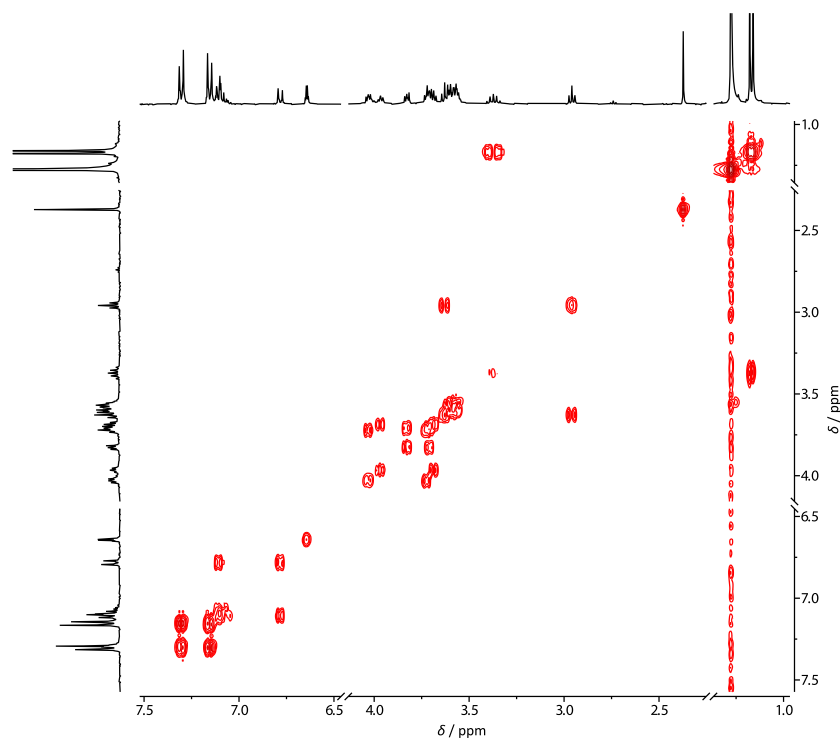


Fig. S4 COSY (¹H, ¹H) spectrum (400 MHz, 298 K, 2.0 mM, CD₃CN) recorded of the dumbbell **D**. The areas omitted contain H₂O and solvent residual peaks.

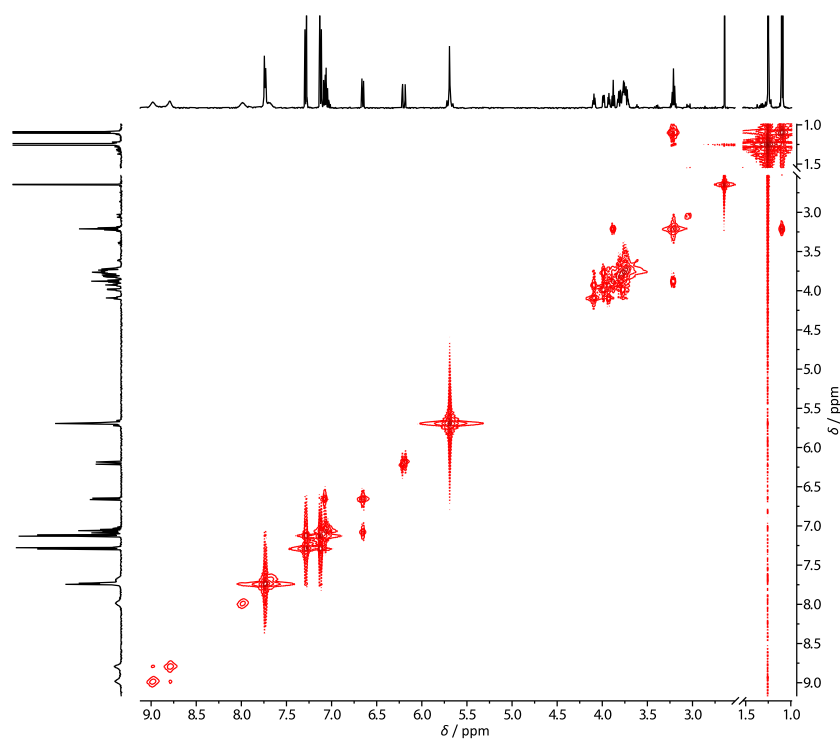


Fig. S5 COSY (¹H, ¹H) spectrum (400 MHz, 298 K, 2.0 mM, CD₃CN) recorded of the [2]rotaxane **R⁴⁺**. The area omitted contains H₂O and solvent residual peaks.

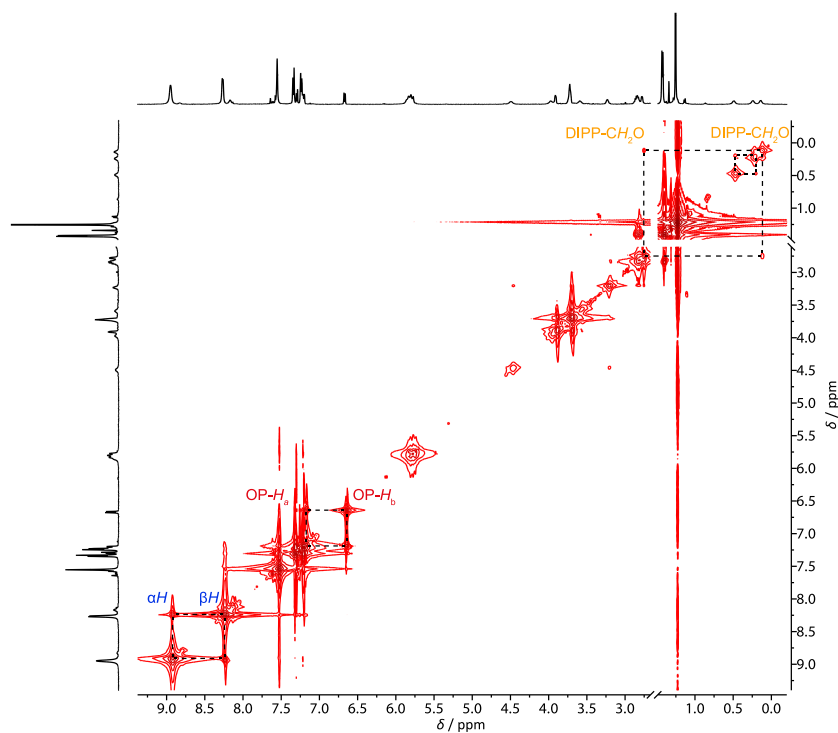


Fig. S6 COSY (¹H, ¹H) spectrum (500 MHz, 253 K, 2.0 mM, CD₃CN) recorded of the oxidised [2]rotaxane R•DIPP⁶⁺. The COSY spectrum and the ¹H NMR spectrum on the axes were recorded 8 min after the addition of ten equiv. of TBPASbCl₆ to unoxidised R⁴⁺. The area omitted contains H₂O and solvent residual peaks.

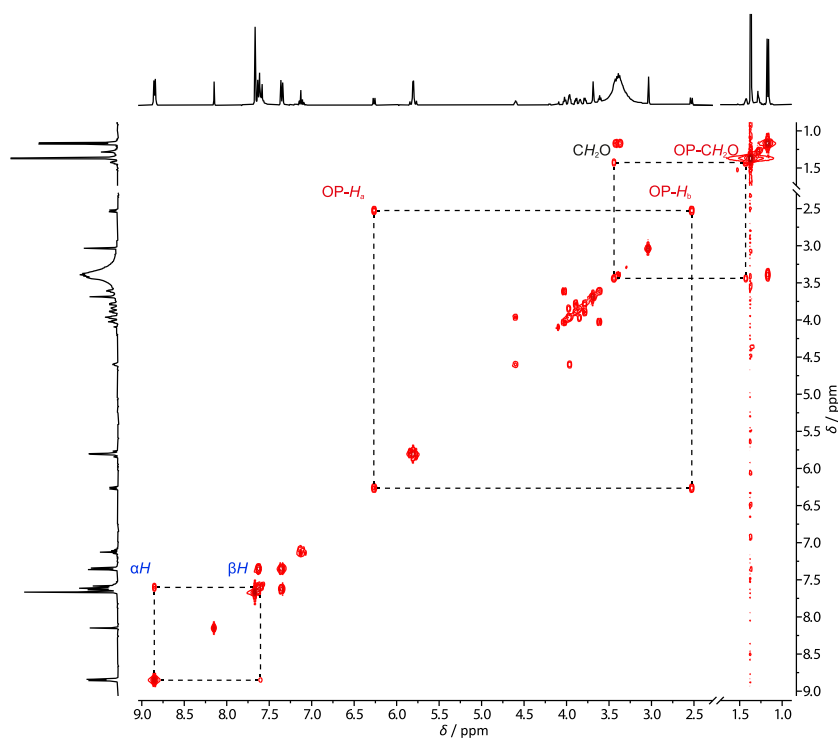


Fig. S7 COSY (¹H, ¹H) spectrum (400 MHz, 298 K, 2.0 mM, CD₃CN) recorded of the oxidised [2]rotaxane R•OP⁶⁺. The COSY spectrum and the ¹H NMR spectrum on the axes were recorded 155 and 80 min after the addition of ten equiv. of TBPASbCl₆ to unoxidised R⁴⁺. The area omitted contains solvent residual peaks.

6 Electrochemical characterisation

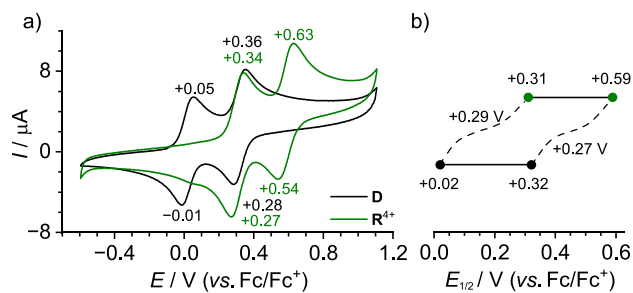
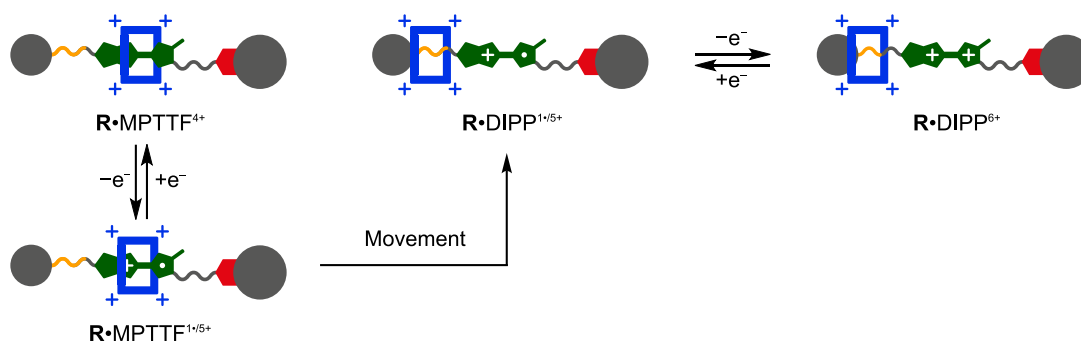


Fig. S8 (a) Cyclic voltammograms of the dumbbell **D** (black) and the [2]rotaxane **R**⁴⁺ (green). The measurements were carried out at 298 K in nitrogen-purged MeCN solutions containing 0.1 M *n*-Bu₄N⁺PF₆⁻ with a scan rate of 100 mV s⁻¹. (b) Correlation diagram showing the difference in half-wave potentials ($E_{1/2}$) between **D** and **R**⁴⁺.



Scheme S2 Cartoon representation of the redox processes and movements to produce **R**•DIPP⁶⁺ by electrochemical oxidation of **R**•MPTTF⁴⁺.

7 ^1H NMR kinetic experiment carried out on R^{6+}

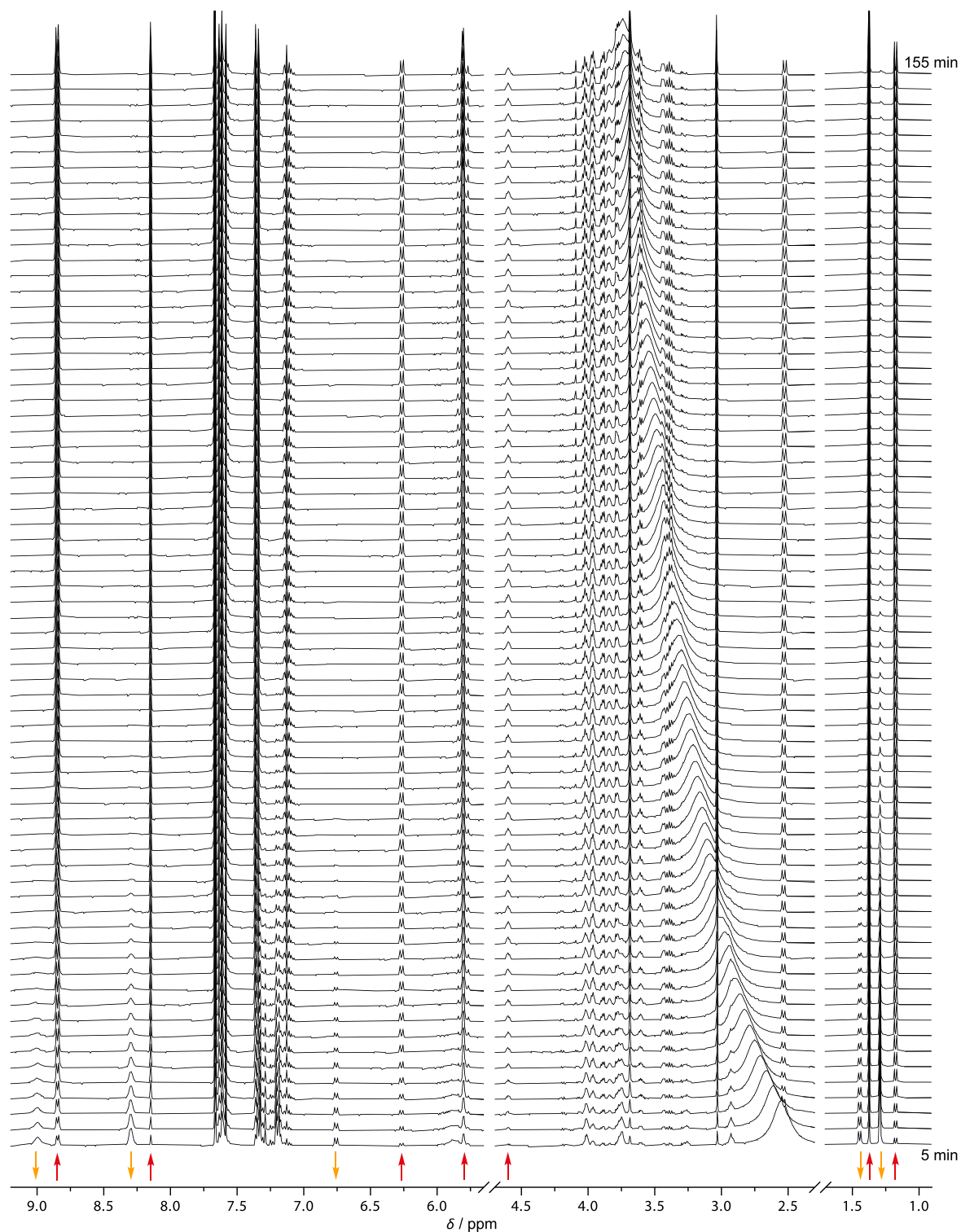


Fig. S9 Partial ^1H NMR spectra (400 MHz, 298 K, CD_3CN , 2 mM) showing the conversion of $\text{R}\cdot\text{DIPP}^{6+}$ into $\text{R}\cdot\text{OP}^{6+}$, where the first spectrum was recorded ca. 5 min after the addition of 10 equiv. of TBPASbCl_6 , while the subsequent spectra were recorded approximately every two min. Signals that do not interfere with other signals or solvent residual signals during the full timeframe of the kinetic experiment are marked with an arrow. Increasing signals for $\text{R}\cdot\text{OP}^{6+}$ are marked with \uparrow and decreasing signals for $\text{R}\cdot\text{DIPP}^{6+}$ are marked with \downarrow . Areas omitted contain the solvent residual signal or no signals. The area from 0.9 to 1.7 ppm is scaled in intensity.

8 First-order analysis of the NMR kinetic experiment

To quantify the barrier for the movement of CBPQT⁴⁺ across the MPTTF²⁺ dication in **R**⁶⁺ in the forward direction (i.e. **R**•DIPP⁶⁺ → **R**•OP⁶⁺), the data from the ¹H NMR kinetic experiment (Fig. S9) was analysed by assuming that the movement initially follows first-order kinetics.

Prior to the integration of the signals, phase and baseline corrections were performed on all the recorded spectra. The TMS signal was used as an internal standard and normalised to 200. All signals that do not overlap with any other signals at the beginning of the experiment were integrated and normalised to the number of hydrogens present and used as probes. A plot of $\ln I$ against t was made for each probe (two examples are shown in Fig. S10), and only data points (n) at the beginning of the experiment, where the reverse process is yet not occurring to any significant extent, were used for linear regression. The data points have been fitted by the best straight line (black lines) indicating that first-order kinetics are in operation.

The k_1 values and the corresponding free energies of activation^{S9} $\Delta G^\ddagger(k_1)$ were obtained directly from the slope of these straight lines. Only lines with $R^2 \geq 0.90$ (Table S1) were used to calculate average k_1^{av} and $\Delta G^\ddagger(k_1^{\text{av}})$ values. Errors on the rate constants and the free energies of activation were calculated based on Koumura *et al.*^{S10} with $\Delta T = 0.2$ K and $\Delta I = 0.05\%$. The number of data points (n), the R^2 value of the linear regression, the k_1 and the $\Delta G^\ddagger(k_1)$ values are also collected in Table S1.

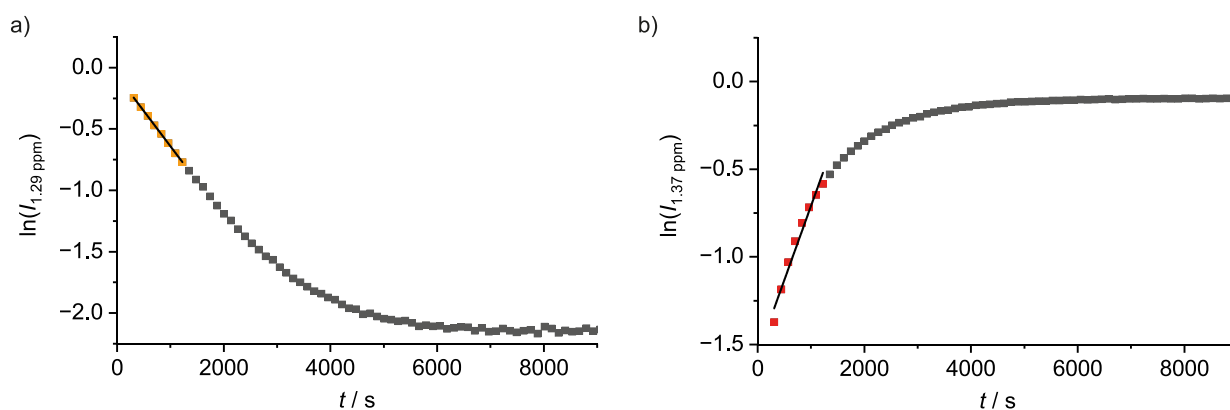


Fig. S10 Plots of $\ln I$ against t at 298 K for the movement of CBPQT⁴⁺ across the MPTTF²⁺ barrier in **R**⁶⁺, in the direction from **R**•DIPP⁶⁺ to **R**•OP⁶⁺, where I is the integral of the signal in question. In (a) the decreasing signal at 1.29 ppm was used as probe and in (b) the increasing signal at 1.37 ppm was used as probe. In both cases, the eight data points have been fitted by the best straight line (black line), giving correlation coefficients (R^2) of 1.00 and 0.97, respectively, indicating that first-order kinetics are in operation. The slope of each line corresponds to the rate constant k_1 for the movement of CBPQT⁴⁺ over the MPTTF²⁺ unit in **R**⁶⁺, according to the relationship $\ln I = k_1 t$.

Table S1 k_1 and ΔG^\ddagger_1 values for each probe in $\mathbf{R}\cdot\text{DIPP}^{6+}$ (top) and $\mathbf{R}\cdot\text{OP}^{6+}$ (bottom) at 298 K in CD_3CN . The number of data points (n) used for the linear regression and the R^2 value for the linear regression are also shown for each probe.

	δ / ppm	Assignment	n	$k_1 / 10^{-4} \text{ s}^{-1}$	$\Delta G^\ddagger_1 / \text{ kcal mol}^{-1}$	R^2
$\mathbf{R}\cdot\text{DIPP}^{6+}$	1.29	$\text{C}(\text{CH}_3)_3$	8	5.75 ± 1.84	21.9 ± 0.2	1.00
	1.44	$\text{CH}(\text{CH}_3)_2$	8	4.93 ± 1.92	22.0 ± 0.2	1.00
	6.76	$\text{OP-}H_b$	8	9.13 ± 3.36	21.6 ± 0.2	0.96
	8.30	$\text{CBPQT}^{4+}\text{-}\beta H$	8	6.71 ± 2.31	21.8 ± 0.2	1.00
	9.00	$\text{CBPQT}^{4+}\text{-}\alpha H$	8	7.61 ± 3.03	21.7 ± 0.2	0.99
$\mathbf{R}\cdot\text{OP}^{6+}$	1.17	$\text{CH}(\text{CH}_3)_2$	8	8.31 ± 2.76	21.7 ± 0.2	0.96
	1.37	$\text{C}(\text{CH}_3)_3$	8	8.46 ± 2.80	21.7 ± 0.2	0.97
	4.60	NCH_2	8	14.1 ± 8.12	21.4 ± 0.2	0.93
	5.79+5.82	$\text{CBPQT}^{4+}\text{-N}^+\text{CH}_2$	8	5.47 ± 2.37	21.9 ± 0.3	0.97
	8.15	pyrrole- αH	8	6.15 ± 2.48	21.8 ± 0.2	0.98
	8.85	$\text{CBPQT}^{4+}\text{-}\alpha H$	8	8.80 ± 2.87	21.6 ± 0.2	0.95

9 Determination of rate constants by the numerical method

To quantify the rate constants for the movement of CBPQT^{4+} across the MPTTF^{2+} dication in \mathbf{R}^{6+} in both the forward (k_1) and backward (k_{-1}) direction, the complete data set from the ^1H NMR kinetic experiment (Fig. S9) was used to numerically solve the two coupled differential equations Eq. 1 and Eq. 2.

$$\frac{dI_{\text{OP}}}{dt} = k_1 I_{\text{DIPP}} - k_{-1} I_{\text{OP}} \quad \text{Eq. 1}$$

$$\frac{dI_{\text{DIPP}}}{dt} = k_{-1} I_{\text{OP}} - k_1 I_{\text{DIPP}} \quad \text{Eq. 2}$$

Prior to the integration of the signals, phase and baseline corrections were performed on all the recorded spectra. The TMS signal was used as an internal standard and normalised to 200. Only signals that did not interfere with other signals or solvent residual signals during the full timeframe of the kinetic experiment were used as probes.

To obtain a numerical solution to the differential equations, one signal for the $\mathbf{R}\cdot\text{DIPP}^{6+}$ isomer and one signal for the $\mathbf{R}\cdot\text{OP}^{6+}$ isomer were used as probes (Table S2). All signals were combined in any possible way (Table S3) by using one increasing signal ($\mathbf{R}\cdot\text{OP}^{6+}$) and one decreasing signal ($\mathbf{R}\cdot\text{DIPP}^{6+}$) as the probes. All integrals are normalised to the number of hydrogens present in each signal to obtain data which are proportional to the concentration of each isomer. For every combination, the conservation of mass is checked, as the increase in I_{OP} should be equal to the

decrease in I_{DIPP} . This is done by adding I_{OP} to I_{DIPP} (i.e. $I_{total} = I_{OP} + I_{DIPP}$) for each combination in every recorded spectrum and then plotting I_{total} as a function of time. All combinations of I_{total} against t having a slope less than $9.99 \cdot 10^{-5}$ in the linear fit were considered as having conservation of mass and were used to solve the two coupled differential equations Eq. 1 and Eq. 2.

Setting up the data file

All increasing signals (I_{OP}) and decreasing signals (I_{DIPP}) were named A–G and A–E, respectively. Each combination of sets of I_{OP} and I_{DIPP} (e.g. A and A) were saved as separate .csv files (i.e. AA.csv) including three columns with time (header = time), normalised integral of I_{OP} (header = op) and normalised integral of I_{DIPP} (header = dipp). All data files were saved in a folder containing the MATLAB function file before every combination was run using the function.

S1.1 MATLAB Function

```
function [k,fval,t,num] = ParamFittingV2(~)
close all
clear
```

Import of data

```
data1 = readtable('AA.csv');
data1 = data1(1:end,:);

data.time = data1.time;
data.op = smooth(data1.op);
data.dipp = smooth(data1.dipp);
```

Defining variables

```
%Value from first-order analysis and/or guessed k value
k1 = 6.30;
k2 = 7.84E-05;

%Number of iterations
m1 = 50;
```

The minimisation

```
if ~exist('k0','var')
    K0 = ([k1,k2]);
```

```

else
    K0 = k0;
end
bestFVal = inf;
M = m1;
ti = tic;
f = waitbar(0, 'Please wait');
for i = 1:M
    option = optimoptions('fmincon','Display','off','StepTolerance',1e-12);
    K = 1e-4*(randn(size(K0))+K0); % ITERATES FROM 0-M TIMES THE GUESSED k-VALUES
    A = [0,0];
    b = -0.1;
    [k,Fval] = fmincon(@(K) errorest(K,data),K,A,b,[],[],[0,0],[[],[]],option);
    if Fval<bestFVal
        bestFVal = Fval;
        bestK = k;
    end
    WallT = round((toc(ti))/i*M-toc(ti));
    waitbar(i/M,f,"Solving problem "+WallT+"s to go")
end
close(f);
k=bestK;
fval=bestFVal;

%plot solution
y0 =[data1.op(1),data.dipp(1)];
[t,num] = ode23s(@(t,y) diffeq(t,y,k),data.time,y0);

figure(1)
plot(t,num(:,1),'b')
hold on
plot(t,num(:,2),'g')

plot(data1.time,data1.op,'b--')
plot(data.time,data1.dipp,'g--')

figure(2)
subplot(1,2,1)
plot(t,num(:,1))
hold on
plot(data.time,data1.op)
title('op')
xlabel('time / s')
ylabel('Int')

subplot(1,2,2)
plot(t,num(:,2))

```

```

hold on
plot(data.time,data1.dipp)
title('dipp')
xlabel('time / s')
ylabel('Int')
function err = errorest(k,data)
y0 =[data.op(1),data.dipp(1)];
[~,num] = ode23s(@(t,y) diffeq(t,y,k),data.time,y0);
err1 = norm(num(:,1)-data.op)^2;
err2 = norm((num(:,2)-data.dipp))^2;
err = sqrt(err1+err2);

function [dydt] = diffeq(~,y,k) %Defining the coupled differential equations
dydt = zeros(2,1);
dydt(1) = k(1)*y(2)-k(2)*y(1); % Change in OP isomer
dydt(2) = k(2)*y(1)-k(1)*y(2); % Change in DIPP isomer

```

Published with MATLAB® R2020b

The MATLAB function uses the `fmincon` function for non-linear optimisation. The optimisation is evaluated based on the `fval` value, that is defined as the value of the objective function. In this case the objective function is $\sqrt{(\sum(\text{err}(n)))}$, where $\text{err}(n) = \text{norm}(\text{calc}(n)-\text{exp}(n))^2$, with n being the number of different isomers present. Hence a smaller `fval` value, equals a better fit between the numerical solution and the experimental data.

9.1 Results from MATLAB calculation on R^{6+} at 298 K

For the oxidised [2]rotaxane R^{6+} , the seven increasing and five decreasing signals listed in Table S2 and Fig. S11 were used to derive the two rate constants k_1 and k_{-1} .

Table S2 Different ^1H NMR signals used as probes to derive the rate constants k_1 and k_{-1} by the numerical method. Probes marked in red are related to $\text{R}\cdot\text{OP}^{6+}$, while probes marked in orange are related to $\text{R}\cdot\text{DIPP}^{6+}$.

$\text{R}\cdot\text{OP}^{6+}$			$\text{R}\cdot\text{DIPP}^{6+}$		
Probe	δ / ppm	Assignment	Probe	δ / ppm	Assignment
A	1.17	$\text{CH}(\text{CH}_3)_2$	A	1.29	$\text{C}(\text{CH}_3)_3$
B	1.37	$\text{C}(\text{CH}_3)_3$	B	1.44	$\text{CH}(\text{CH}_3)_2$
C	4.60	NCH_2	C	6.76	OP-H_b
D	5.79 and 5.82	$\text{CBPQT}^{4+}\text{-N}^+\text{CH}_2$	D	8.30	$\text{CBPQT}^{4+}\text{-}\beta\text{H}$
E	6.27	OP-H_a	E	9.00	$\text{CBPQT}^{4+}\text{-}\alpha\text{H}$
F	8.15	pyrrole- αH	-	-	-
G	8.85	$\text{CBPQT}^{4+}\text{-}\alpha\text{H}$	-	-	-

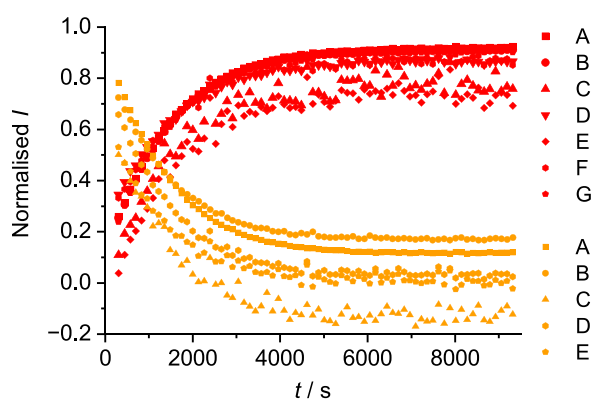


Fig. S11 Plot of the normalised I of the selected probes for $\mathbf{R}\cdot\text{OP}^{6+}$ (red) and $\mathbf{R}\cdot\text{DIPP}^{6+}$ (orange) against t .

All combinations of probes (Table S2) which showed conservation of mass were used to obtain numerical solutions using the MATLAB function described above. The solutions (*i.e.* k_1 and k_{-1}) and the associated f_{val} values are listed in Table S3, and examples of the fitted data for the AA and BD combination of probes are shown in Fig. S12.

Table S3 Rate constants, k_1 and k_{-1} together with their corresponding f_{val} values obtained by the numerical method. The letters represent the different probes: The first letter (red) represents a probe from $\mathbf{R}\cdot\text{OP}^{6+}$, and the second letter (orange) represents a probe from $\mathbf{R}\cdot\text{DIPP}^{6+}$.

Combinations	$k_1 / 10^{-4} \text{ s}^{-1}$	$k_{-1} / 10^{-5} \text{ s}^{-1}$	f_{val}
AA	6.30	7.84	0.085
AB	6.34	8.49	(0.543)
AC	19.4	3.02	(1.510)
AD	7.47	2.18	0.207
AE	10.1	0.25	(0.881)
BA	6.31	8.07	0.100
BB	6.32	8.56	(0.523)
BC	18.8	2.90	(1.484)
BD	7.11	1.41	0.154
BE	11.1	1.35	(0.907)
CA	6.50	9.42	0.124
CB	6.67	10.8	(0.628)
CC	21.5	4.38	(1.580)
CD	7.62	1.82	0.273
CE	13.7	3.93	(1.089)
DA	6.04	12.0	(0.779)
DB	6.04	12.8	0.194
DC	12.9	2.38	(1.053)
DD	6.79	6.44	(0.569)
DE	7.37	0.80	0.106

EA	6.49	8.42	0.222
EB	6.43	8.56	(0.794)
EC	30.3	7.87	(1.837)
ED	7.87	0.89	0.441
EE	15.3	4.89	(1.329)
FA	6.18	11.7	(0.670)
FB	5.92	11.5	0.113
FC	13.4	2.24	(1.069)
FD	7.35	6.89	0.479
FE	7.63	0.23	0.146
GA	6.35	7.78	0.058
GB	6.45	8.69	(0.588)
GC	20.1	3.29	(1.557)
GD	7.27	1.26	0.218
GE	12.8	1.30	(1.001)

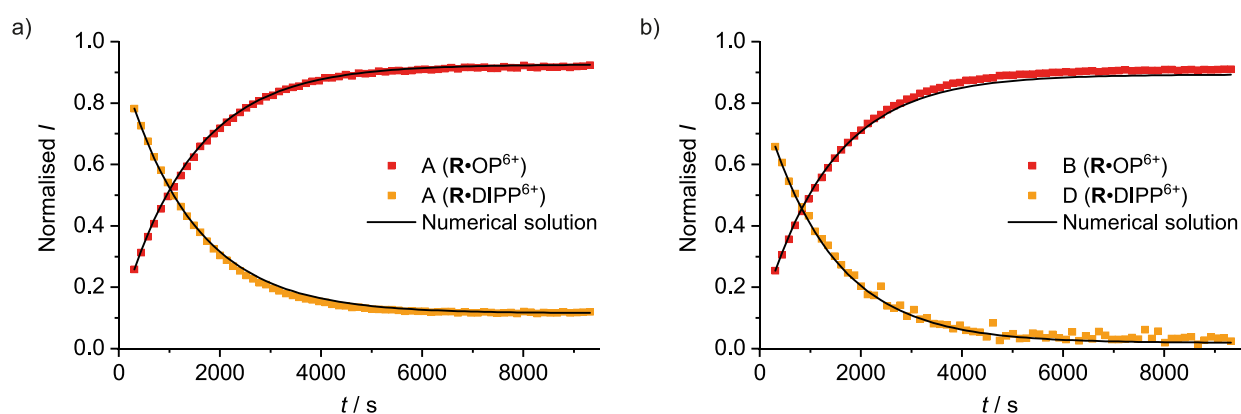


Fig. S12 Representative plots of experimental data and their corresponding numerical solutions for (a) the combination of A ($\text{R}\cdot\text{OP}^{6+}$, red) and A ($\text{R}\cdot\text{DIPP}^{6+}$, orange) and (b) the combination of B ($\text{R}\cdot\text{OP}^{6+}$, red) and D ($\text{R}\cdot\text{DIPP}^{6+}$, orange).

Based on the f_{val} values, only combinations with a value less than 0.50 were used in the calculation of an average value for the rate constants (*i.e.* k_1^{av} and k_{-1}^{av}), and the corresponding averages Gibbs free energies of activation^{S9} (*i.e.* $\Delta G^\ddagger(k_1^{\text{av}})$ and $\Delta G^\ddagger(k_{-1}^{\text{av}})$). These results are listed in Table S4.

Table S4 Average rate constants (k_1^{av} and k_{-1}^{av}) and corresponding Gibbs free energies of activation ($\Delta G^\ddagger(k_1^{\text{av}})$ and $\Delta G^\ddagger(k_{-1}^{\text{av}})$) for the movement of CBPQT⁴⁺ across the MPTTF²⁺ unit in the [2]rotaxane R^{6+} .

	$k_1^{\text{av}} / 10^{-4} \text{ s}^{-1} \text{ }^a$	$k_{-1}^{\text{av}} / 10^{-4} \text{ s}^{-1} \text{ }^a$	$\Delta G^\ddagger_1 / \text{kcal mol}^{-1} \text{ }^b$	$\Delta G^\ddagger_{-1} / \text{kcal mol}^{-1} \text{ }^b$
R^{6+}	6.91 ± 1.04	0.54 ± 0.08	21.8 ± 0.1	23.3 ± 0.1

^a Errors on the k_1^{av} and k_{-1}^{av} values were estimated to be $\pm 15\%$. ^b Errors on the $\Delta G^\ddagger(k_1^{\text{av}})$ and $\Delta G^\ddagger(k_{-1}^{\text{av}})$ values were calculated from Koumura et al.^{S10} with $\Delta T = 0.2 \text{ K}$.

10 ¹H NMR and ¹³C NMR spectra

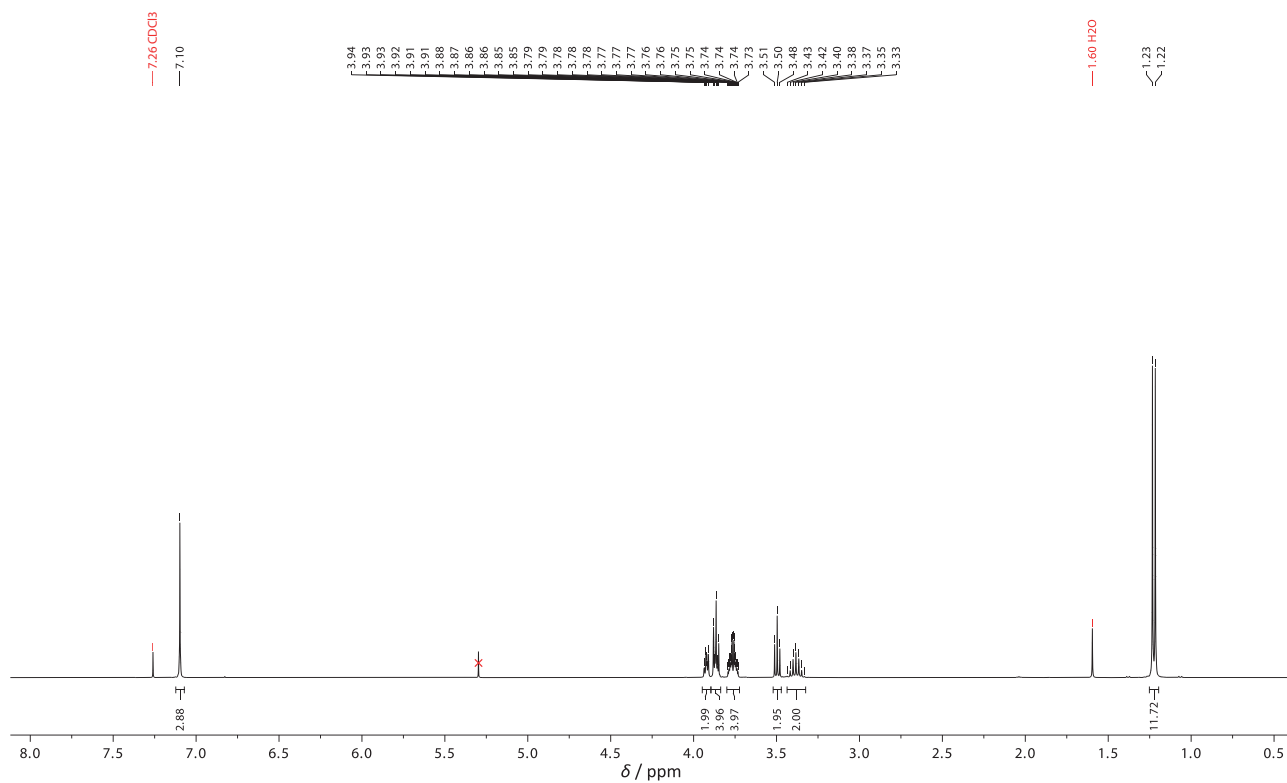


Fig. S13 ¹H NMR spectrum (400 MHz, 298K, CDCl₃) recorded of compound **2**.

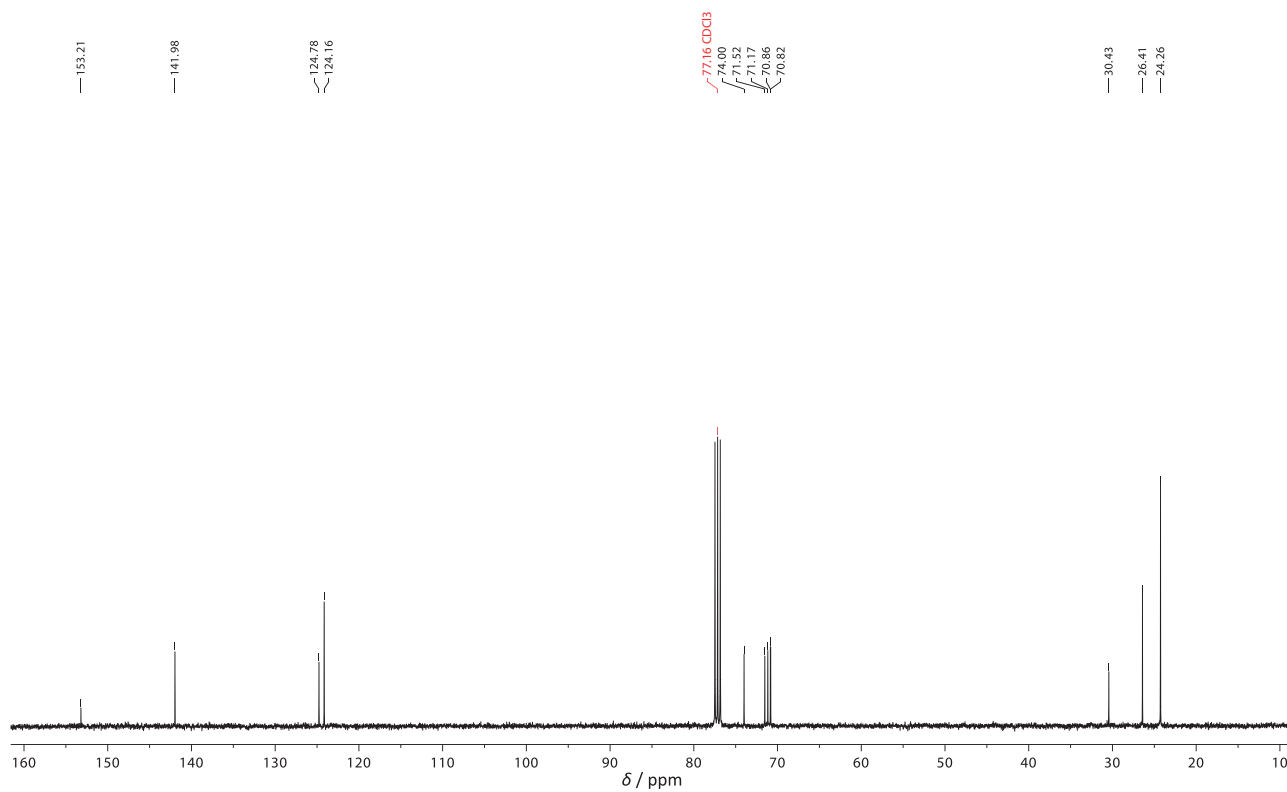


Fig. S14 ¹³C NMR spectrum (100 MHz, 298K, CDCl₃) recorded of compound **2**.

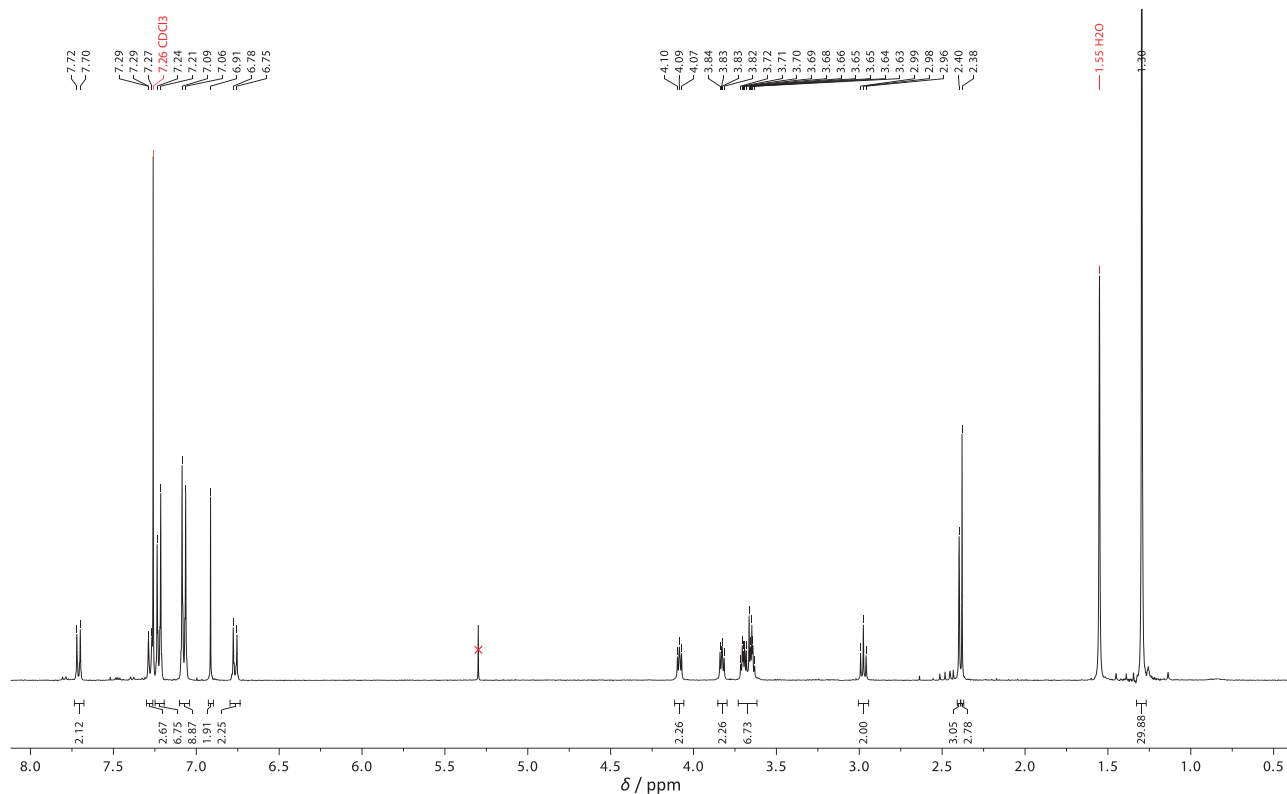


Fig. S15 ¹H NMR spectrum (400 MHz, 298K, CDCl₃) recorded of compound 5.

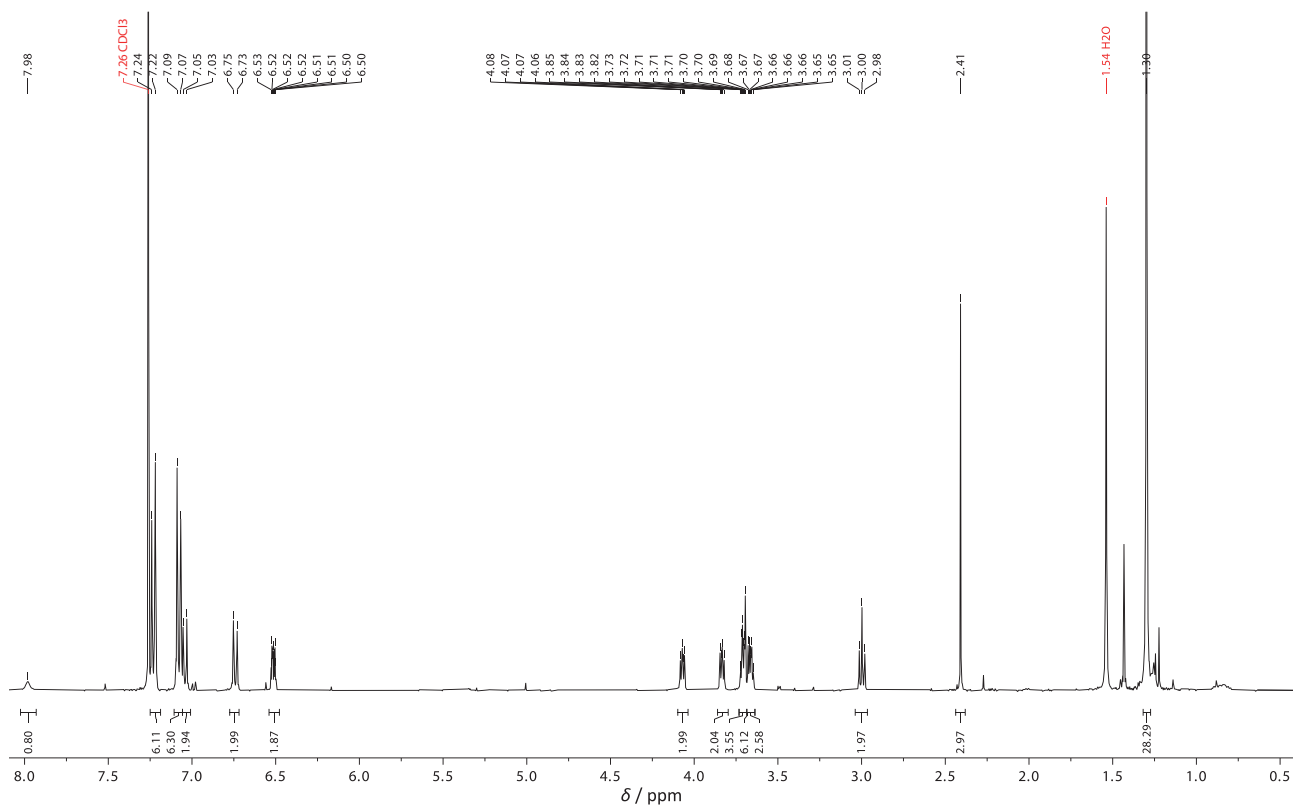


Fig. S16 ¹H NMR spectrum (400 MHz, 298K, CDCl₃) recorded of compound 6.

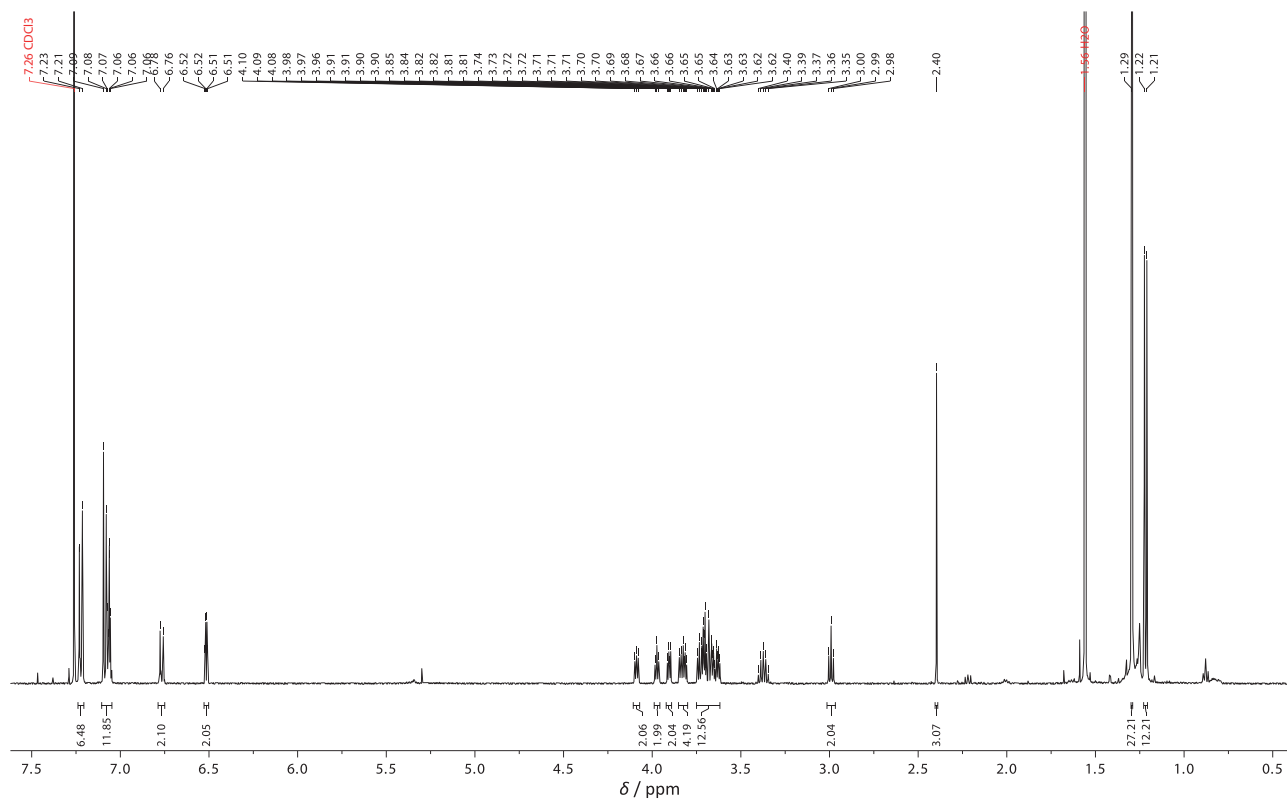


Fig. S17 ¹H NMR spectrum (500 MHz, 298K, CDCl₃) recorded of the dumbbell D.

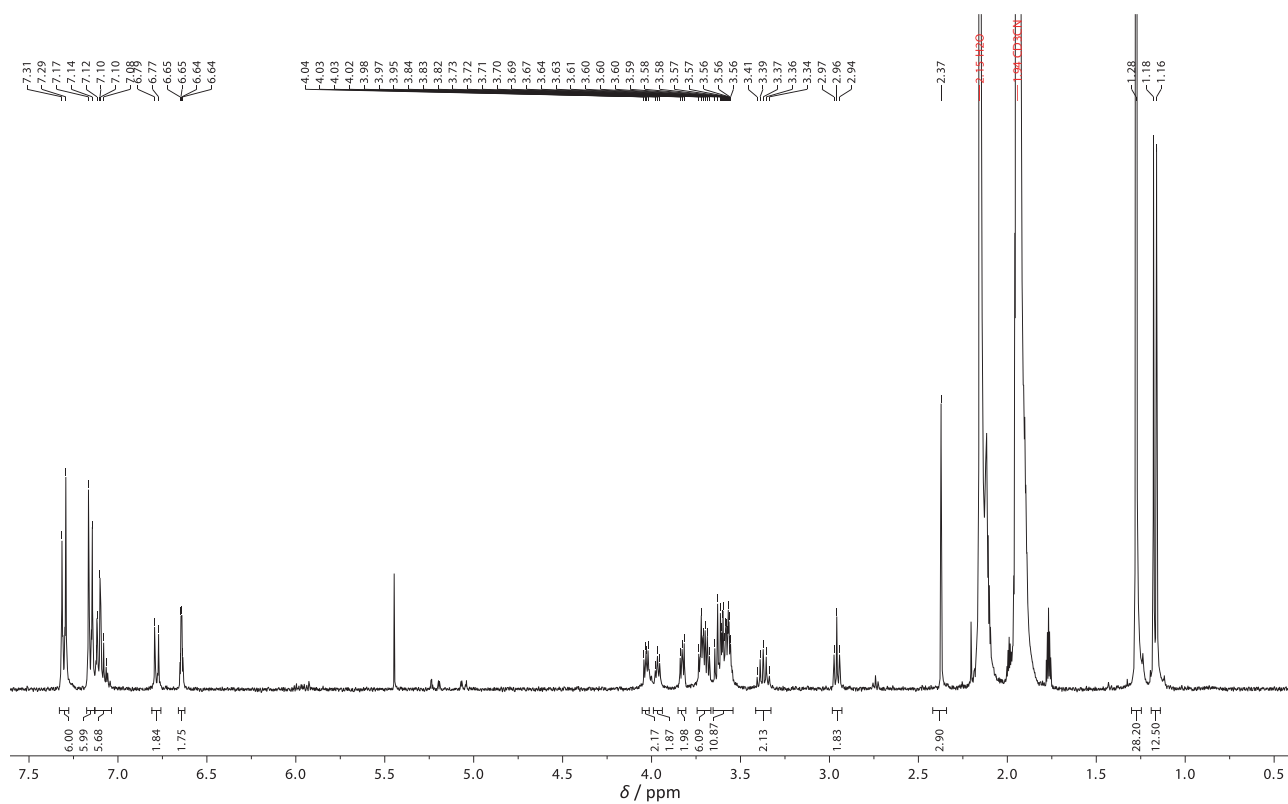


Figure S18 ¹H NMR spectrum (500 MHz, 298K, CD₃CN) of dumbbell D.

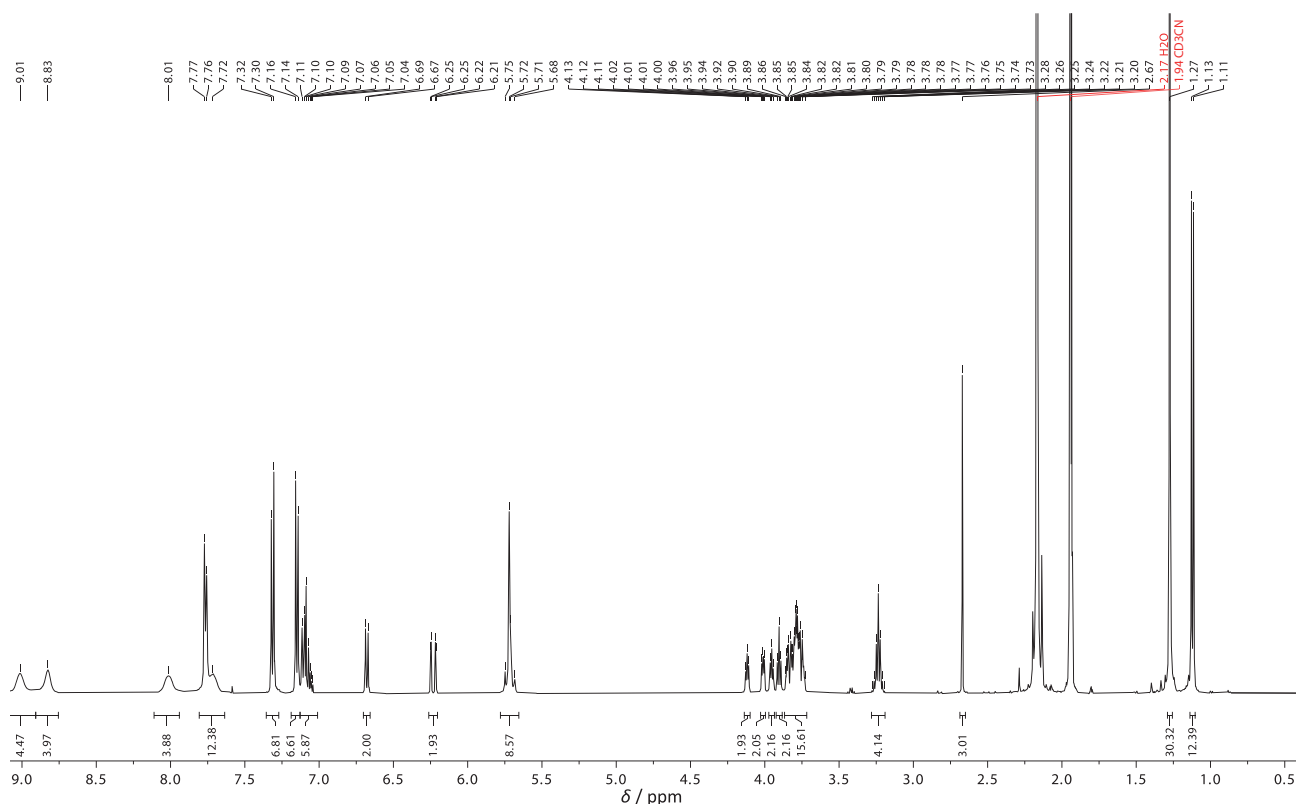


Fig. S19 ^1H NMR spectrum (500 MHz, 298K, CD_3CN) recorded of the [2]rotaxane **R**•4PF₆.

11 References

- S1. T. Ikeda and M. Higuchi, *Tetrahedron*, 2011, **67**, 3046.
- S2. L. J. O'Driscoll, S. S. Andersen, M. V. Solano, D. Bendixen, M. Jensen, T. Duedal, J. Lycoops, C. van der Pol, R. E. Sørensen, K. R. Larsen, K. Myntman, C. Henriksen, S. W. Hansen and J. O. Jeppesen, *Beilstein J. Org. Chem.*, 2015, **11**, 1112.
- S3. J.-P. Collin, F. Durola, J. Lux and J.-P. Sauvage, *Angew. Chem. Int. Ed.*, 2009, **48**, 8532.
- S4. (a) P. L. Anelli, P. R. Ashton, R. Ballardini, V. Balzani, M. Delgado, M. T. Gandolfi, T. T. Goodnow, A. E. Kaifer, D. Philp, M. Pietraszkiwicz, L. Prodi, M. V. Reddington, A. M. Z. Slawin, N. Spencer, J. F. Stoddart, C. Vicent and J. Williams David, *J. Am. Chem. Soc.*, 1992, **114**, 193; (b) M. Asakawa, W. Dehaen, G. L'Abbé, S. Menzer, J. Nouwen, F. M. Raymo, J. F. Stoddart and D. J. Williams, *J. Org. Chem.*, 1996, **61**, 9591.
- S5. H. E. Gottlieb, V. Kotlyar and A. Nudelman, *J. Org. Chem.*, 1997, **62**, 7512.
- S6. Compound **2** has previously been used as a starting material,^{S2} but no experimental procedure was reported.
- S7. The signal is overlapping with the H₂O signal, but from the spectrum recorded after 155 min the signal is visible.
- S8. (a) M. Jensen, R. Kristensen, S. S. Andersen, D. Bendixen and J. O. Jeppesen, *Chem. Eur. J.*, 2020, **26**, 6165; (b) R. Kristensen, M. S. Neumann, S. S. Andersen, P. C. Stein, A. H. Flood and J. O. Jeppesen, *Org. Biomol. Chem.*, 2022, **20**, 2233.

- S9. The ΔG^\ddagger value was calculated using the relationship $\Delta G^\ddagger = RT \ln(kh/k_B T)$, where R is the gas constant, T is the absolute temperature, k is the rate constant, h is Planck's constant and k_B is the Boltzmann constant.
- S10. N. Koumura, E. M. Geertsema, M. B. Van Gelder, A. Meetsma and B. L. Feringa, *J. Am. Chem. Soc.*, 2002, **124**, 5037.